



HAL
open science

Products from the Oxidation of Linear Isomers of Hexene

Frédérique Battin-Leclerc, Anne Rodriguez, Benoit Husson, Olivier Herbinet, Pierre Alexandre Glaude, Zhandong Wang, Zhanjun Cheng, Fei Qi

► **To cite this version:**

Frédérique Battin-Leclerc, Anne Rodriguez, Benoit Husson, Olivier Herbinet, Pierre Alexandre Glaude, et al.. Products from the Oxidation of Linear Isomers of Hexene. *Journal of Physical Chemistry A*, 2014, 118, pp.673-683. 10.1021/jp4107102 . hal-01022632

HAL Id: hal-01022632

<https://hal.science/hal-01022632v1>

Submitted on 10 Jul 2014

HAL is a multi-disciplinary open access archive for the deposit and dissemination of scientific research documents, whether they are published or not. The documents may come from teaching and research institutions in France or abroad, or from public or private research centers.

L'archive ouverte pluridisciplinaire **HAL**, est destinée au dépôt et à la diffusion de documents scientifiques de niveau recherche, publiés ou non, émanant des établissements d'enseignement et de recherche français ou étrangers, des laboratoires publics ou privés.

Products from the Oxidation of Linear Isomers of Hexene

Frédérique Battin-Leclerc^{1}, Anne Rodriguez¹, Benoit Husson¹, Olivier Herbinet¹,
Pierre-Alexandre Glaude¹, Zhandong Wang², Zhanjun Cheng², Fei Qi²*

¹Laboratoire Réactions et Génie des Procédés, Université de Lorraine, CNRS,
ENSIC, BP 20451, 1 rue Grandville, 54000 Nancy, France

²National Synchrotron Radiation Laboratory, University of Science and Technology of China, Hefei,
China

Abstract

The experimental study of the oxidation of the three linear isomers of hexene was performed in a quartz isothermal jet-stirred reactor (JSR) at temperatures ranging from 500 to 1100 K including the negative temperature coefficient (NTC) zone, at quasi-atmospheric pressure (1.07 bar), at a residence time of 2 s and with dilute stoichiometric mixtures. The fuel and reaction product mole fractions were measured using online gas chromatography. In the case of 1-hexene, the JSR has also been coupled through a molecular-beam sampling system to a reflectron time-of-flight mass spectrometer combined with tunable synchrotron vacuum ultraviolet photoionization.

* E-Mail : Frederique.Battin-Leclerc@univ-lorraine.fr,
Tel : 33 3 83175125, Fax : 33 3 83378120

A difference of reactivity between the three fuels which varies with the temperature range has been observed and is discussed according to the changes in the possible reaction pathways when the double bond is displaced. An enhanced importance of the reactions via the Waddington mechanism and of those of allylic radicals with HO₂ radicals can be noted for 2- and 3-hexenes compared to 1-hexene.

Keywords: Jet-stirred reactor, linear isomers of hexene, low-temperature oxidation, alkene oxidation, hydroxycyclic ethers, unsaturated hydroperoxides.

Introduction

Octane numbers show an important influence of the position of the double bond on the knocking properties of linear alkenes: research octane number is 76.4, 92.7 and 94, for 1-hexene, 2-hexene and 3-hexene, respectively¹. To our knowledge there are still deficiencies in the models for low-temperature oxidation of isomers of linear alkenes²⁻⁴, especially in the prediction of the observed products. In addition to this, the only available data for model validation are mostly those obtained in rapid compression machines (RCM) at low and intermediate temperatures⁵⁻⁶.

Concerning 1-alkenes, representative of the compounds present in gasoline, i.e. containing at least 5 atoms of carbon, Ribaucour et al.⁷ measured ignition delay times of 1-pentene in a RCM (600-900 K) and proposed a kinetic model. Another model for the oxidation of this species has been proposed by Mehl et al.³ validated using the same experimental data⁵. Touchard et al.⁸ studied ignition delay times of 1-pentene in a shock tube proposing a new model. The oxidation of 1-pentene has also been studied in a flow tube (600-900 K)⁹. Tanaka et al.⁶ have measured the pressure profile during the combustion of the 3 linear isomers of heptene in a RCM at 827 K. Mehl et al.¹⁰ have measured shock tube ignition delay times (990-1770 K) for 1- and 2-pentenenes and proposed a kinetic model which is also able to reproduce data at low temperature.

As far as hexenes are concerned, the high-temperature oxidation of 1-hexene has been studied by Yahyaoui et al. in a JSR between 750 and 1200 K¹¹ at 10 atm and in a shock tube at higher temperatures¹¹⁻¹². The proposed kinetic model under-estimates the reactivity below 850 K. Vanhove et al.⁵ measured cool flame and ignition delay times, as well as the formation of pre-ignition products, for the 3 linear isomers of hexene in a RCM (600-900 K). Using a version of EXGAS software extended to alkenes, Touchard et al.² proposed mechanisms for the oxidation of 1-pentene and 1-hexene. Based on this last work, and using quantum mechanical calculations to gain a better insight into the isomerizations of alkenyl radicals, Bounaceur et al.⁴ proposed models for the three isomers of hexene and heptene validated using experimental results available in the literature^{5,6,8}. The study of Mehl et al.¹⁰ on low to high temperature ignition delay times also concerns the three linear isomers of hexene.

Experimental Methods

Experiments were performed using two similar spherical quartz JSR operating at constant temperature, pressure, and residence time. This type of reactor is well adapted for kinetic studies: the gas phase inside the reactor is well stirred and concentration is homogenous¹³ with

a limited effect of possible wall reactions¹⁴. Stirring is achieved by four turbulent jets located at the center of the sphere. Both JSRs consist of a quartz sphere (volume $\approx 90 \text{ cm}^3$) attached to a quartz annular preheating zone in which the gas temperature is increased up to the reactor temperature. The gas mixture residence time inside the annular preheater is very short compared to its residence time inside the reactor (about a few percent). Both the spherical reactor and the annular preheating zone are heated by means of Thermocoax resistances rolled up around the wall. Reaction temperature is measured with a thermocouple located inside the intra-annular space of the preheating zone; the extremity of the thermocouple is on the level of the injection jets. Pressure is measured using a MKS Baratron Type 631 pressure transducer. The accuracy is $\pm 1\%$. Temperatures are measured using type K thermocouples with an accuracy of $\pm 2 \text{ K}$. The uncertainty in the residence time is mainly due to the uncertainty in the gas flow rates. The accuracy of the flow controllers provided by Bronkhorst is $\pm 1\%$ which leads to an uncertainty of $\pm 0.1 \text{ s}$ in the residence time.

The JSR used in the National Synchrotron Radiation Laboratory (NSRL) in Hefei (China) is coupled via a molecular beam to a NSRL's reflectron time-of-flight mass spectrometer. The second JSR is located in the Laboratoire Réactions et Génie des Procédés in Nancy (France) where the outlet gas was analysed by gas chromatography.

JSR and gas chromatography (Nancy)

The same types of reactor and analytical methods have also been recently used to study the oxidation of linear¹⁵ and cyclic¹⁶ alkanes. Reaction products were analyzed online using three gas chromatographs via a heated transfer line (consisting in an inert-coated copper tube) kept at 423 K. The first chromatograph was fitted with a carbosphere packed column and two detectors: a thermal conductivity detector (TCD) for oxygen and carbon oxides and a flame ionization detector (FID) for C_1 - C_2 hydrocarbons. The second chromatograph was fitted with a Plot Q capillary column and a FID coupled with a methanizer to analyse molecules from methane to reaction products containing up to 5 carbon atoms and 1 or 2 oxygen atoms maximum. A third one was fitted with a HP-5 capillary column and a FID and was used for the quantification of molecules which contain at least 5 carbon atoms. Helium was used as carrier gas in these three chromatographs. Identification and calibration of gaseous species were performed by injecting standard gaseous mixtures provided by Air Liquide and Messer. Identification of species was also performed with an on-line chromatograph also fitted with a Plot Q or a HP-5 column, but coupled with a mass spectrometer. The quantification of the species which were not available

for calibration was performed using the effective carbon number method. This method is based on the response of the detector (FID) as a function of the structure of the molecule. While water and hydrogen peroxide were identified as products, it was not possible to quantify them. The limit of detection for the FID was about 0.1 ppm for hydrocarbon species. For the TCD, the limit of detection depended on the thermal conductivities of the carrier gas and of the solutes. Estimated uncertainties of the species mole fractions were about $\pm 5\%$ with the online analysis of oxygen and C₁-C₂ hydrocarbons, about 20% for formaldehyde, and about $\pm 10\%$ for the analysis of other species.

The gases used in Nancy were provided by Messer (purity of 99.95%). Gas flows were controlled by Bronkhorst mass flow controllers. The isomers of hexene were provided by ALFA AESAR, with a purity of 98% for 1-hexene, 99% for 2-hexene and 97% for 3-hexene.

JSR and SVUV photoionization mass spectrometry (Hefei)

In the case of 1-hexene, additional species identifications were performed using a reflectron time-of-flight mass spectrometer (RTOF-MS) with photo-ionization by synchrotron radiation. The reactor was coupled to the low pressure photo-ionization chamber through a lateral fused silica cone-like nozzle which was inserted in the spherical part. The tip of the cone was pierced by a 50 μm orifice. A nickel skimmer with a 1.25 mm diameter aperture was located 15 mm downstream from the sampling nozzle. The sampled gases formed a molecular beam, which was intersected perpendicularly with synchrotron vacuum ultraviolet light. The ion signal was then detected with the RTOF-MS, which was installed in the photo-ionization chamber vertically. Additional details about this experimental apparatus are available in Ref. ¹⁷. Note that raw signals of all the compounds were normalized by the ion signal obtained for argon (m/z 40) at a photon energy of 16.6 eV which acted as an internal standard.

Gases were provided by Nanjing Special Gas Factory Co. Ltd. Purities of argon and oxygen were 99.99% and 99.999% respectively. 1-hexene was purchased from Aladdin Reagent (Shanghai) Co. Ltd. with a purity of 99%.

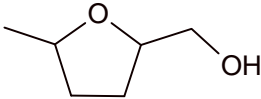
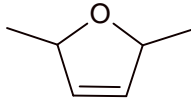
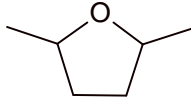
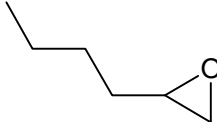
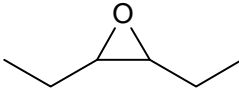
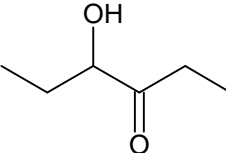
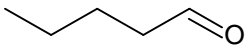
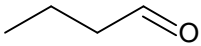
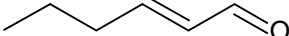
Reactivity of the Three Isomers

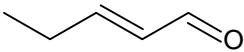
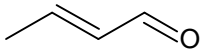
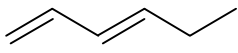
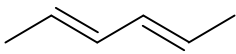
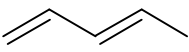
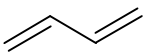
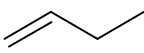
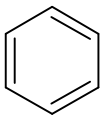
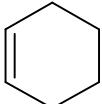
Experiments were performed at a constant pressure of 1.07 bar, at a residence time of 2 seconds, at temperatures ranging from 500 to 1100 K under stoichiometric conditions. The fuel was diluted in helium in Nancy and in argon in Hefei (1-hexene mole fraction of 0.01 and of 0.02 for a few

specified experiments). This high dilution was used to avoid that the exothermicity of the reaction perturbs the homogeneity in temperature inside the reactor.

Figure 1 presents the evolution with temperature of the consumption of the three linear isomers of hexene, as well as of the formation of some main products. Gas chromatography quantifications have been made for carbon oxides, all the hydrocarbon products from methane to C₆ species, and oxygenated compounds from formaldehyde and methanol to C₆ compounds including aldehydes, ketones and cyclic ethers (see supplementary material). Note that only very small amounts of acetic acid have been detected. The structure of the major analysed species including at least four atoms of carbon is presented in Table 1.

Table 1: Name, global formula, structure and molecular weight of the main products analysed by gas chromatography, containing at least four atoms of carbon.

| Name | Global formula | Structure | Molecular weight (g.mol ⁻¹) |
|--|---|--|--|
| 2-methyl, 5-hydroxymethyl- tetrahydrofuran | C ₆ H ₁₂ O ₂ |  | 116.16 |
| dimethyl-dihydrofuran | C ₆ H ₁₀ O |  | 98.14 |
| 2,5-dimethyl- tetrahydrofuran | C ₆ H ₁₂ O |  | 100.16 |
| butyl-oxirane | C ₆ H ₁₂ O |  | 100.16 |
| 2,3-diethyl-oxirane | C ₆ H ₁₂ O |  | 100.16 |
| 3-hydroxy-4-hexanone | C ₆ H ₁₂ O ₂ |  | 116.16 |
| pentanal | C ₅ H ₁₀ O |  | 86.13 |
| butanal | C ₄ H ₈ O |  | 72.11 |
| 2-hexenal | C ₆ H ₁₀ O |  | 98.14 |

| | | | |
|----------------|-------------|--|-------|
| 2-pental | C_5H_8O |  | 84.12 |
| 2-butenal | C_4H_6O |  | 70.09 |
| 1,3-hexadiene | C_6H_{12} |  | 84.16 |
| 2,4-hexadiene | C_6H_{12} |  | 84.16 |
| 1,3-pentadiene | C_5H_8 |  | 68.12 |
| 1,3-butadiene | C_4H_6 |  | 54.09 |
| 1-butene | C_4H_8 |  | 56.11 |
| benzene | C_6H_6 |  | 78.11 |
| cyclohexene | C_6H_{10} |  | 84.16 |

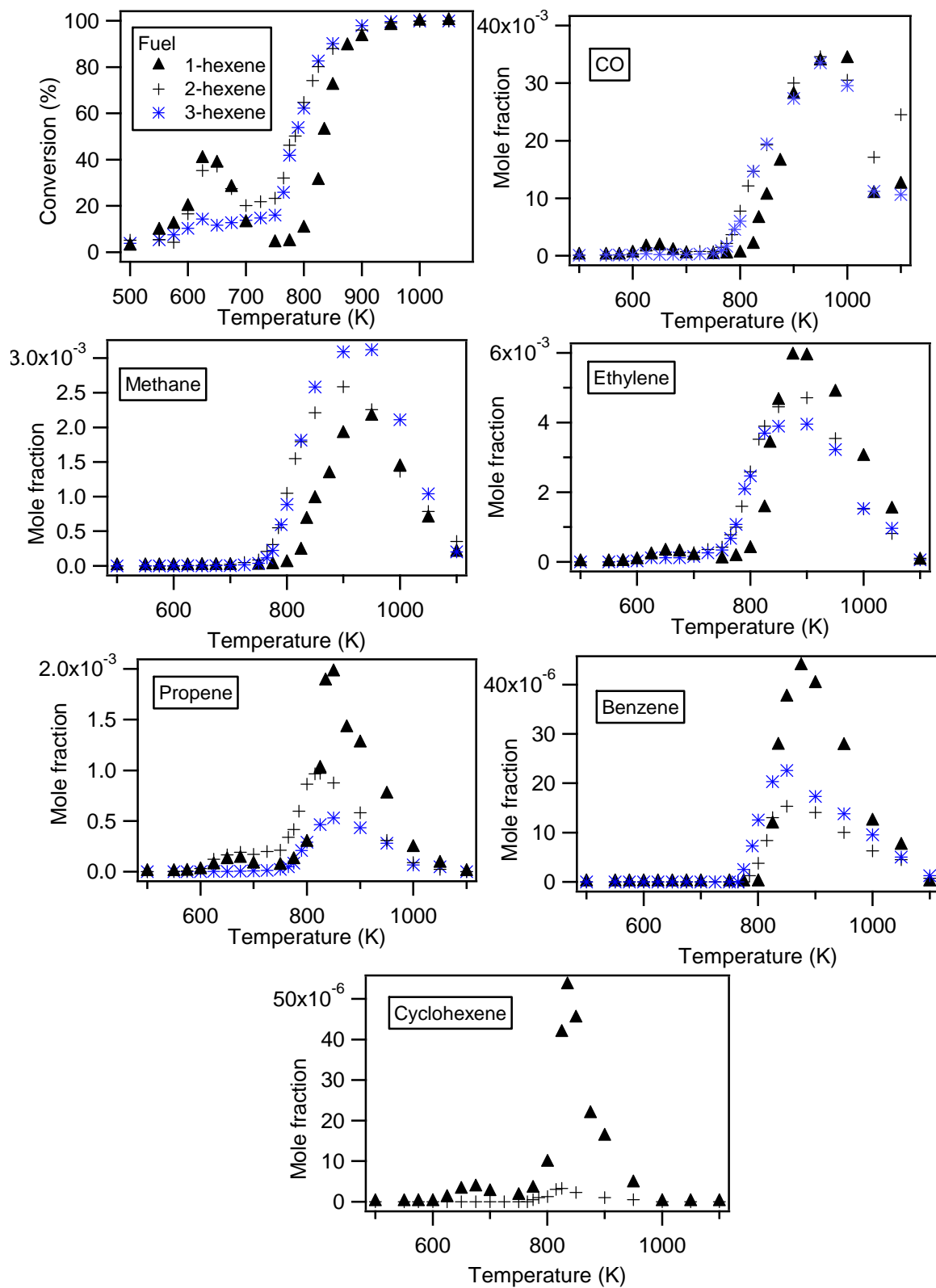


Figure 1. Comparison between the three isomers of hexene for the fuel conversion and the formation of CO, methane, ethylene, propene, benzene and cyclohexene.

In Figure 1, three distinct zones of reactivity can be clearly observed. In a first zone, from 500 to 700 K, 1-hexene is the most reactive fuel closely followed by 2-hexene, and 3-hexene is by far the least reactive isomer. This is in agreement with the ranging of reported octane numbers (see introduction). However the octane numbers of 1-hexene (76.4) and 2-hexene (92.7) would have suggested a larger difference of reactivity compared to what is observed here. The results of Vanhove et al.⁵ obtained in a RCM also indicate 1-hexene as the most reactive isomer, closely followed by 2-hexene, with 3-hexene being by far the least reactive. In this first zone, 1-hexene and 2-hexene have a well marked NTC zone. The extent of this NTC zone is more limited for 2-hexene than for 1-hexene. No NTC zone can be seen for 3-hexene. The same trend as that observed for the global reactivity can be seen when looking at the formation of CO or propene.

The ranking between reactivity for the 3 isomers obtained in the second zone, from 700 to 850 K is more unexpected, especially when compared to the RCM results of Vanhove et al.⁵ showing the same reactivity ranking between isomers over all the studied temperature range. Note that our JSRs were operated close to atmospheric pressure while RCM experiments were performed between 8 and 11 bar. There is a well known influence of pressure on the equilibrium of the addition reactions which can shift the temperature zones in which some specific reactions are of importance and explain differences in reactivity ranking between isomers. In this study, in the intermediate temperature zone, 2-hexene is the most reactive isomer closely followed by 3-hexene, with the reactivity of 1-hexene being then significantly less important. Note also that from 700 to 800 K, the formation of the main products shown in Figure 1 is rather weak. Only a small amount of ethylene is formed from 2- and 3-hexenes and of propene from 2-hexene. Above 750 K, the formation of methane is more important from 2- and 3-hexenes than from 1-hexene.

Above 850 K, the consumptions of the three isomers are almost complete and are very similar. The formation of ethylene and propene which can be obtained by β -scission decomposition is the largest for 1-hexene, followed by 2-hexene. These decompositions are more difficult for the radicals derived from 3-hexene explaining their lowest formation. Note that 1-hexene-5-yl radical, which can be obtained from 1-hexene, can decompose by breaking a C-C bond to give propene and an allyl radical. 1-Hexene-6-yl radical, which can also be obtained from 1-hexene, can cyclicize to give cyclohexene, explaining why this species has a significantly higher formation in the case of 1-hexene as shown in Figure 1. Certainly dehydrogenations from cyclohexene are partly the cause of the high production of benzene observed from 1-hexene oxidation.

Figure 2 presents the selectivity of the products formed in significant amount for the temperature of the maximum of reactivity of 1-hexene (625 K) and for one after the NTC zone (825 K). At 825K, the major products are carbon monoxide and small unsaturated species, which are

formed by relatively well-known decomposition channels. At 625K, a large range of oxygenated species are formed by pathways which have not been so well studied¹⁸. Therefore only the global reactivity and the species, the formation of which is important at 625 K, are discussed in details below.

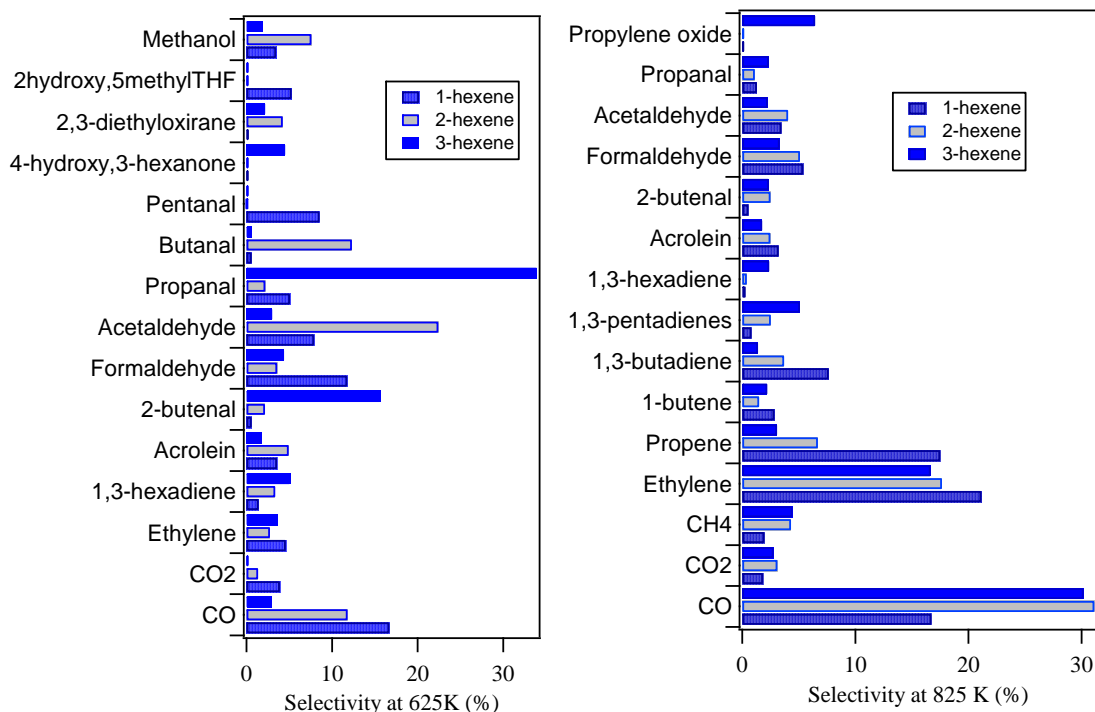


Figure 2. Product selectivity at 625 and 825 K. At 625 K, only the products with a selectivity above 5.3% are shown. At 825 K, only the products with a selectivity above 2.3% are shown.

Discussion about the observed differences in reactivity at low temperature

Figure 3 presents the main reactions which occur during alkene oxidation at low and intermediate temperatures according to previous modeling works^{2,4}. Figure 3 has been drawn for 1-hexene, note that similar pathways can be considered for the two other isomers.

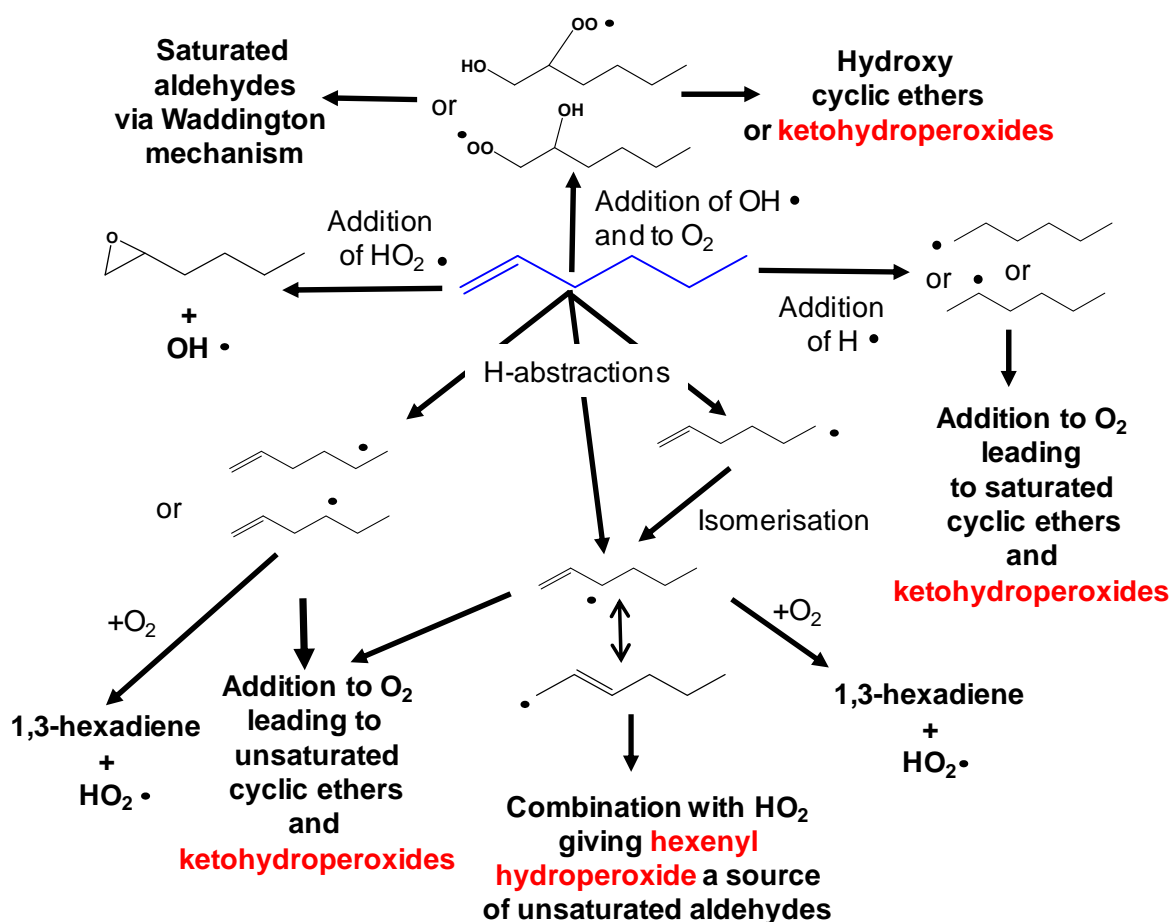


Figure 3. Schematic way of consumption of 1-hexene at low and intermediate temperatures.

Below 800 K, the main reactions consuming linear hexenes are H-abstractions and additions of OH radicals to the double bond, followed by the addition of O_2 molecule producing peroxyhydroxyhexyl radicals. The H-abstractions leading to the resonance stabilized radicals are particularly favored. The additions of H-atoms to form alkyl radicals and of HO_2 radicals to form oxiranes contribute also, but to a smaller extent. The radicals formed in all cases react mainly by addition to an oxygen molecule and can be a source of ketohydroperoxides. Ketohydroperoxides are the branching agents leading to a multiplication of the number of radicals and then their formation promotes considerably the reactivity¹⁹. Therefore the reactivity of a fuel at low temperature varies as a function of its ability to form ketohydroperoxides.

Products deriving from the OH radicals addition to the double bond

Nothing prevents peroxyhydroxyhexyl radicals ($\cdot\text{OOROH}$) to react like alkyl radicals by isomerizations, followed by a second addition to an oxygen molecule, and to be a source of

hydroxycyclic ethers and hydroxyketohydroperoxides promoting the reactivity. However these hydroxycyclic ethers, the formation of which is postulated by models², have never been quantified previously amongst products of alkene oxidation. In the present study the formation of hydroxycyclic ethers (identified as mostly cis and trans 2-methyl,5-hydroxymethyltetrahydrofurans) has been observed in the case of 1-hexene oxidation by gas chromatography. Some channels explaining the formation of five-member ring cyclic ethers from the radical obtained by addition of OH• on the outer atom of carbon of the double bond in 1-hexene are presented in Figure 4. 2-Methyl,5-hydroxymethyltetrahydrofuran is the compound which can certainly be the most easily formed. The evolution with temperature of the mole fraction of the sum of cis and trans 2-methyl,5-hydroxymethyltetrahydrofurans (GC analysis) formed during 1-hexene oxidation is displayed in Figure 5, which presents cyclic ethers and hydroxyketone including 6 atoms of carbon. Note that 2-methyl,5-hydroxymethyltetrahydrofurans are the major five-membered ring cyclic ethers obtained from linear hexene oxidation, with a maximum mole fraction of 77 ppm at 625 K.

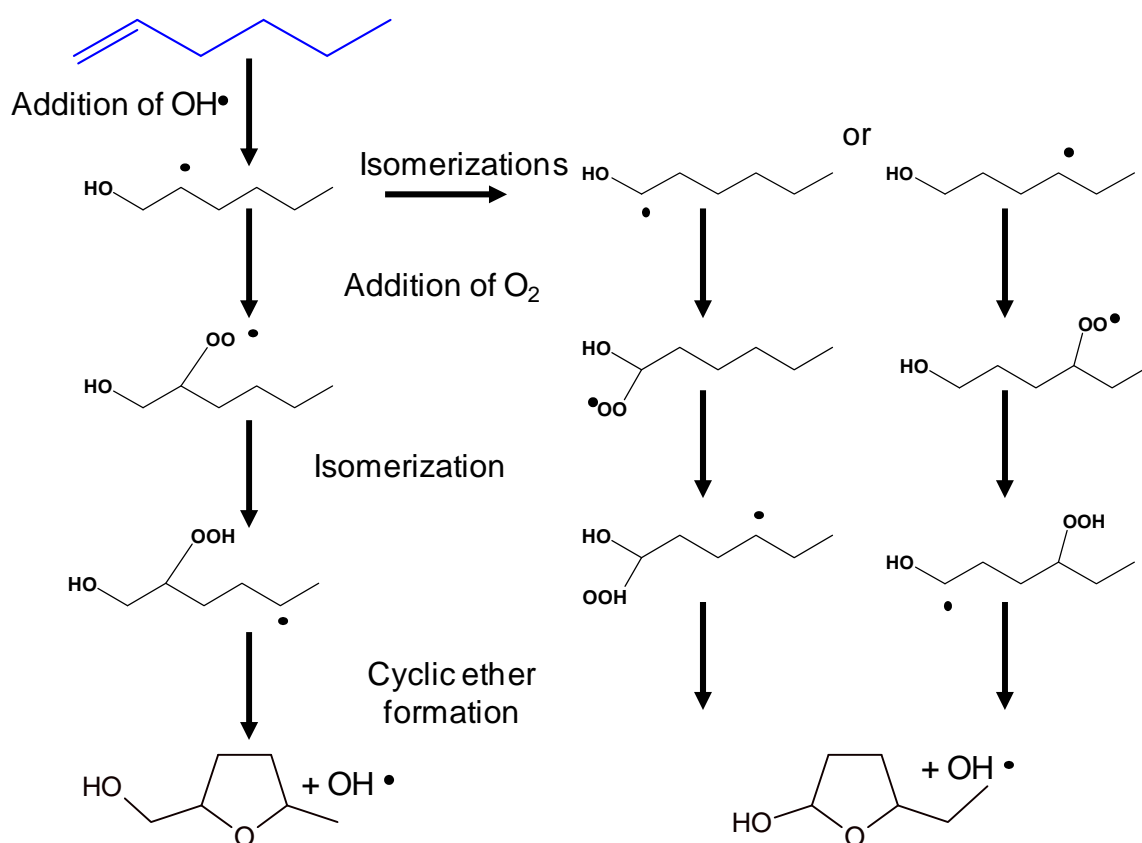


Figure 4. Possible pathways for the formation of five-membered ring cyclic ethers from the addition of OH radicals to the outer atom of carbon of the double bond of 1-hexene.

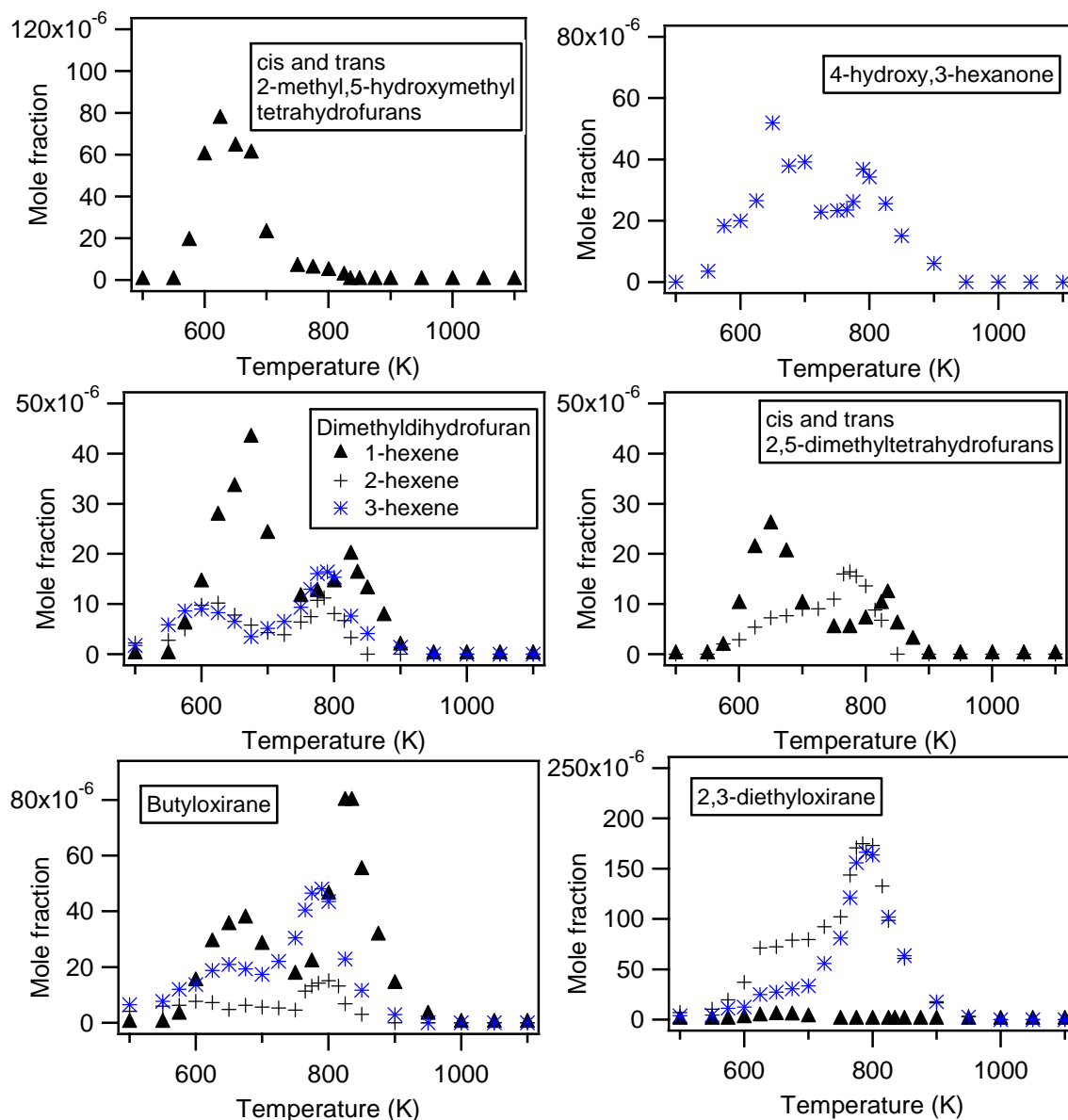


Figure 5. Comparison between the three isomers of hexene for the formation of three- and five-membered ring cyclic ethers and hydroxyketone including 6 atoms of carbon.

A signal at m/z 116 corresponding to hydroxycyclic ethers has been registered in Hefei data. Note that m/z 116 is also the mass corresponding to hexenyl hydroperoxide isomers. Figure 6 presents the results of an experimental sweeping of photon energies from 8.3 to 11.5 eV at m/z 116 and shows an ionization threshold close to 9.22 eV. Zero-point energy corrected adiabatic ionization energies have been calculated from the composite CBS-QB3 method²⁰ using Gaussian03²¹ for hexenyl hydroperoxide and for different possible isomers of hydroxycyclic ethers and are displayed in Table 2.

The calculated value is close to 9.25 eV for hexenyl hydroperoxide, supporting the presence of hexenyl hydroperoxide. However the calculated value for 2-methyl,5-hydroxymethyltetrahydrofuran is lower than 9 eV, indicating that this compound fully decomposes during ionization or has a very low cross section. This would explain why its molecular peak cannot then be observed.

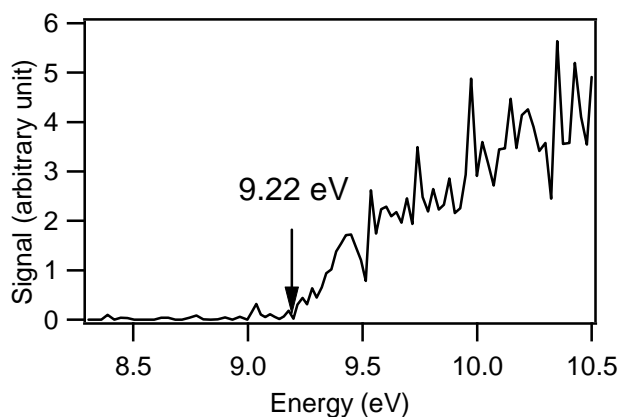
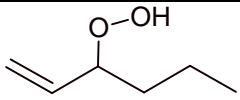
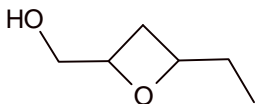
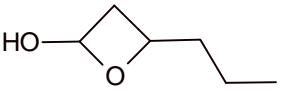
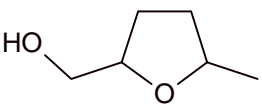
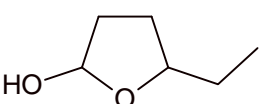
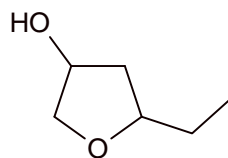


Figure 6. Photoionization efficiency spectra at m/z 116 at a temperature of 625 K in the reactor (1-hexene mole fraction of 0.02).

Table 2: Calculated ionization energies (eV) of most expected isomers for m/z 116 deriving from 1-hexene. Calculations were performed using the composite CBS-QB3 method (20) in Gaussian03 (21).

| Name | | EI (eV/mol) |
|--|--|---------------------------------|
| Hexenylhydroperoxide |  | 9.25 |
| 2-ethyl, 4-hydroxymethyltetrahydrofuran |  | 9.19 (cis), 9.16 (trans) |
| 2-propyl, 4-hydroxytetrahydrofuran |  | 8.72 (cis), 9.57 (trans) |
| 2-methyl, 5-hydroxymethyl tetrahydrofuran |  | 8.98 (cis), 8.88 (trans) |
| 2-ethyl, 5-hydroxy tetrahydrofuran |  | 9.41 (cis), 9.42 (trans) |

2-ethyl,
4-hydroxy
tetrahydrofuran



9.49 (cis), 9.46 (trans)

Looking at the experimental signals presented in Figure 7a for a photon energy of 9.5 eV, the evolution with temperature at m/z 116 has a shape close to that of the usual profile observed for hydroperoxides in our previous studies^{12,17,22}. This profile is characterized by a very sharp peak, as shown in Figure 7a with the signal profile obtained for butylhydroperoxide during *n*-butane oxidation¹⁷. However this signal is very weak and can only be seen for an initial 1-hexene mole fraction of 0.02. Looking at the experimental signals presented in Figure 7b for a photon energy of 10 eV, the evolution with temperature at m/z 116 has a shape closer to other saturated (m/z 100) and unsaturated cyclic (m/z 98) ethers including 6 atoms of carbon. This would indicate that the signal at m/z 116 corresponds also for a large fraction to the hydroxycyclic ethers. This could probably be due to a small presence of 2-ethyl,5-hydroxytetrahydrofuran (calculated ionization threshold close to 9.4 eV), the pathways of formation of which are presented in Figure 4. It is certainly formed in significantly lower amounts than 2-methyl,5-hydroxymethyltetrahydrofuran, explaining why it is not observed by gas chromatography.

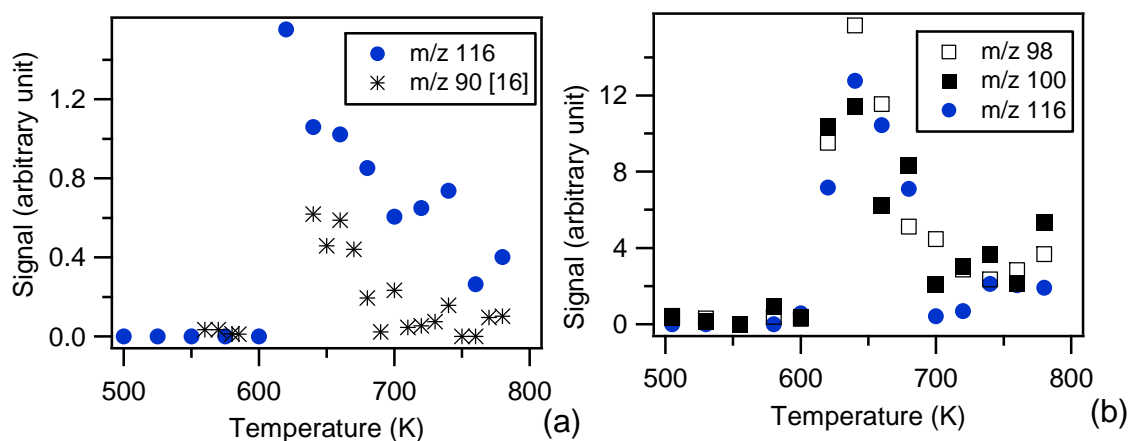


Figure 7. Experimental normalized signals versus temperature obtained during 1-hexene oxidation for (a) m/z 116 (with a photoionization of 9.5 eV and a 1-hexene mole fraction of 0.02) compared with the profile obtained for butylhydroperoxide during *n*-butane oxidation (17) and (b) m/z 98, 100 and 116 (with a photoionization of 10 eV and a 1-hexene mole fraction of 0.01).

A concurrent channel to the isomerizations of peroxyhydroxyhexyl radicals is the so-called Waddington mechanism²³ leading to the formation of OH radicals and two saturated aldehydes:

formaldehyde and pentanal from 1-hexene, acetaldehyde and butanal from 2-hexene, and two molecules of propanal from the symmetric 3-hexene. Figure 8 presents the evolution with temperature of these saturated aldehydes.

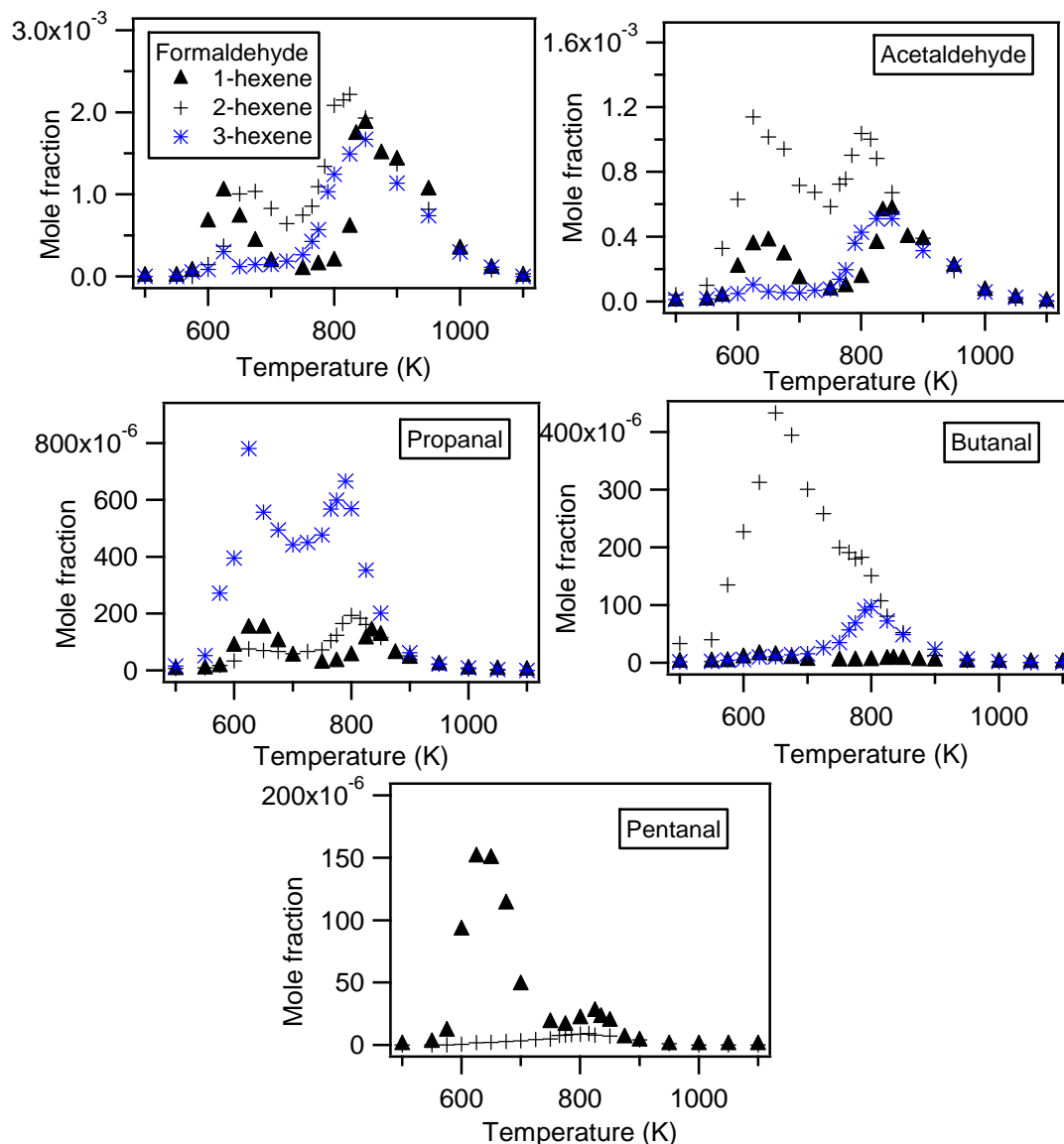


Figure 8. Comparison between the three isomers of hexene for the formation of saturated aldehydes.

It can be observed that 1-pentanal is only formed in the case of 1-hexene. The formations of propanal and butanal are by far the largest in the case of 3-hexene and 2-hexene, respectively. As expected, the formation of acetaldehyde is also the largest in the case of 2-hexene. However this aldehyde is also obtained from 1-hexene since this small species can easily be formed by several other pathways. Below 620 K, the formation of formaldehyde is by far the largest in the case of

1-hexene, as expected. However, here also this small species can easily be formed by several other pathways. This explains why formaldehyde is also significantly formed from 2-hexene from 620 to 800 K. Note that the decomposition of ketohydroperoxides can be also a source of small aldehydes, such as acetaldehyde or formaldehyde.

It is interesting to note that, while the conversion of 1-hexene is the highest at low temperature, pentanal is formed in more limited amounts than the other saturated aldehydes. This would indicate that the Waddington mechanism is less favored for this 1-alkene. The formation of hydroxyketohydroperoxides can then more easily occur. This explains certainly for a part the highest reactivity of this species at very low temperature. It can also be observed in Figure 8 that the formation of propanal is about twice that of butanal, indicating that the Waddington mechanism has the same importance in the case of 2- and 3-hexenes. According to the theoretical calculations of Cord et al.²² for propene, the rate constant of the reaction following the Waddington mechanism is about ten times lower at 700 K when the hydroxyl function is carried by the final carbon atom than in the other case. This would support the importance of the Waddington mechanism to be lower in the case of 1-alkenes. This also probably explains, according to Figure 4, why 2-methyl,5-hydroxymethyltetrahydrofuran is the only hydroxycyclic ether observed by gas chromatography.

Note that a better understanding of the importance of the Waddington mechanism would lead to a better modeling of the low temperature reactivity of large alcohols which can be proposed as biofuels²⁴.

As shown in Figure 5, another type of product which could be derived from the additions of OH radicals to the double bond is observed in significant amounts in the case of 3-hexene: 4-hydroxy,3-hexanone. Its formation from peroxyhydroxyhexyl radicals can certainly occur by pathways similar to those playing a role in the formation of C₆ ketones during the oxidation of *n*-hexane under similar conditions²⁵.

Products deriving from the H-atom abstractions or additions to the double bond

Chemically activated allylic radicals can easily undergo cis/trans isomerizations as shown by Dibble et al.²⁶. However, as discussed by Bounaceur et al.⁴, the rate constants of the isomerizations of the stabilized peroxyalkenyl radicals involving a double bond in their transition state are much lower than those for saturated peroxyalkyl radicals. This is due to the fact that some rotations required in the formation of the cyclic transition state involved to undergo the isomerization are hindered by the presence of the double bond⁴. This means that the formation of unsaturated cyclic ethers or unsaturated ketohydroperoxides is more difficult than that in the case of saturated species. This is

particularly significant when the double bond is at the center of the molecule such as in 3-hexene. It is certainly a reason for the lower reactivity of this species. This also explains why the formation of unsaturated cyclic ethers is much larger for 1-hexene than for 2- and 3-hexenes, as shown in Figure 5. Note also that, for 1-hexene, a weak signal at m/z 130 was obtained in Hefei data corresponding to the mass of the unsaturated C₆ ketohydroperoxides.

The alkylperoxy radicals deriving from the addition of H-atom to the double bond are a source of saturated cyclic ethers. Figure 5 presents the evolution with temperature of 2,5-dimethyltetrahydrofuran, which is the major saturated cyclic ether obtained during *n*-hexane oxidation under similar conditions²⁵.

Discussion about the observed differences in reactivity at intermediate temperature

As discussed by Griffiths et al.²⁷ and by Bahrini et al.²⁸, the chemistry of alkane oxidation at intermediate temperature is triggered by the reactions of HO₂ radicals. In the case of alkanes, HO₂ radicals are obtained mainly from the reactions of alkyl radicals with oxygen to produce conjugated alkenes. Given that HO₂ radicals can then only react by a combination with themselves to give H₂O₂, these reactions can almost be considered as termination steps. Since they directly compete with the pathway leading to ketohydroperoxides, the reactions forming HO₂ radicals are very efficient inhibiting channels.

In the case of alkenes, the picture is very different: HO₂ radicals can also combine with the abundant resonance stabilized allylic radicals to give alkenyl hydroperoxides. With a bond dissociation energy around 43 kcal/mol, hydroperoxides can more easily decompose than H₂O₂ (bond dissociation energy about 51 kcal/mol). This decomposition leads to alkoxy and hydroxyl radicals and then promotes the reactivity in a temperature zone where the branching step through ketohydroperoxides is no more favored due to the enhanced reversibility of the addition to oxygen molecules.

HO₂ radicals are mainly produced from the reactions of alkenyl radicals with oxygen forming conjugated dienes. These dienes can be produced from the abstraction of a H-atom either from an alkenyl radical in which the radical center is carried by a carbon atom in α position from the double bond or from resonance stabilised allylic radicals. The corresponding radicals are shown in Figure 3 for 1-hexene and in Figure 9 for the two other isomers. Note that when they are different, the two mesomer forms of each resonance stabilised allylic radicals are presented. According to Touchard et al.², the rate constant of the first pathway (Figure 9) from an alkenyl radical (activation energy around 2.5 kcal/mol) is much larger than that of the second one from an allylic radical (activation

energy around 15 kcal/mol). On the other hand, the concentration of allylic radicals is much larger than that of other alkenyl radicals.

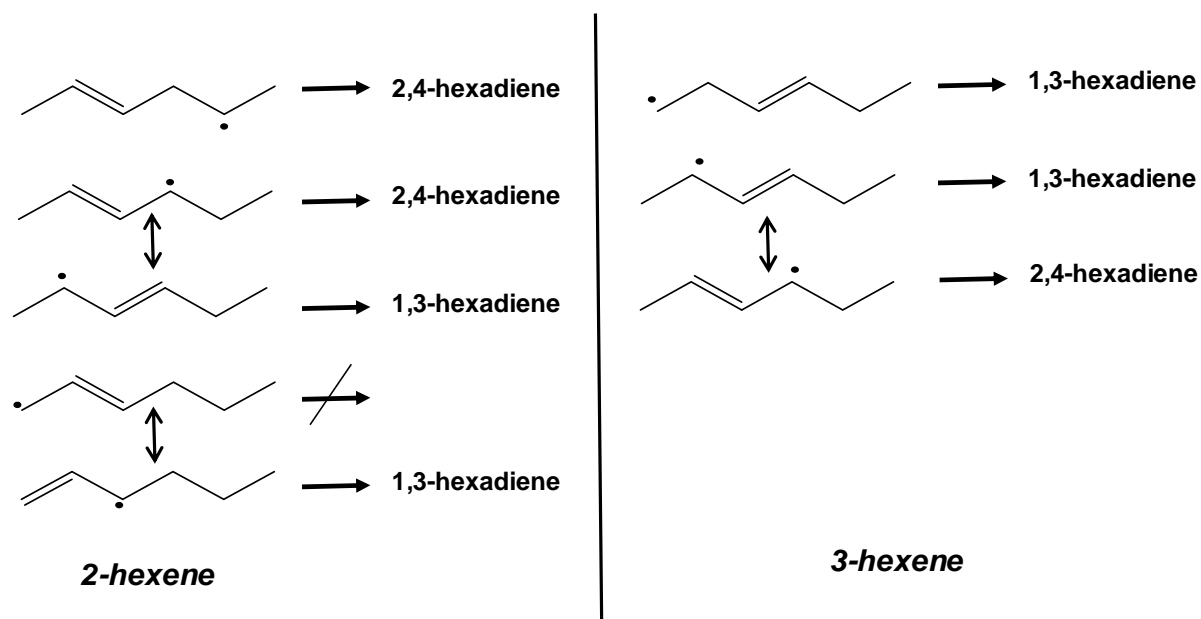


Figure 9. Radicals which can be a source of conjugated hexadienes in the cases of 2-hexene and 3-hexene.

As presented in Figure 10, the formation of HO₂ is much favored in the case of 2- and 3-hexenes, since the formation of the co-products, i.e. the two conjugated hexadienes, is significantly larger. As shown in Figure 3, 1-hexene can only lead to the formation of 1,3-hexadiene and consequently the mole fraction of 2,4-hexadiene observed during its oxidation is very low.

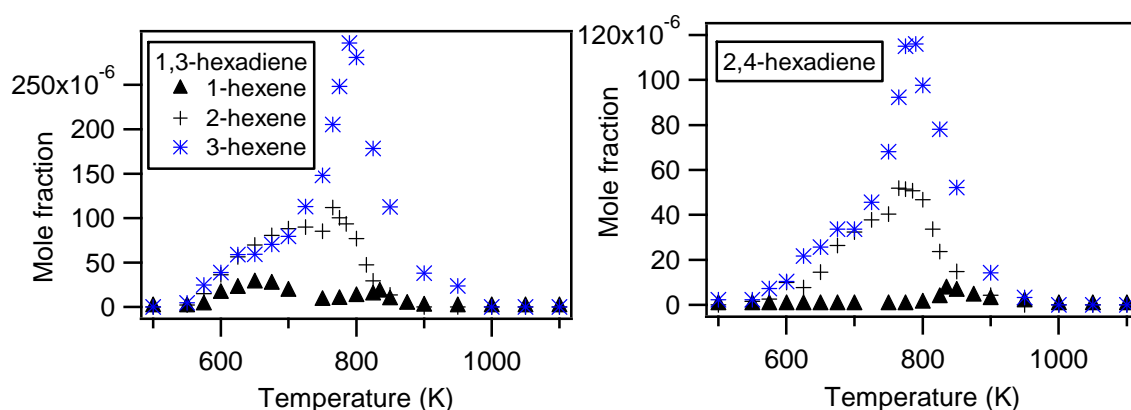


Figure 10. Comparison between the three isomers of hexene for the formation of the two conjugated hexadienes.

The larger formation of 1,3-hexadiene during 2- and 3-hexene oxidation would indicate that dienes are significantly formed from allylic radicals, which can be more easily obtained from 2- and 3-hexenes. The abstraction of two secondary H-atoms, three primary and two secondary H-atoms, and of four secondary H-atoms leads to allylic radicals in the case of 1-, 2- and 3-hexenes, respectively. The fact that the ratio between the amounts formed from 2-hexene and 3-hexene is larger for 2,4-hexadiene than for 1,3-hexadiene is probably due to some contribution of the non-allylic pathway. Note however that this reaction with oxygen is not the limiting one, since the global reactivities of 2- and 3-hexenes are similar above 700 K, while the diene formation is much higher for 3-hexene than for 2-hexene.

The limiting reaction is then most probably the combination of allylic and HO₂ radicals to form a hydroperoxide molecule rapidly decomposing to give a hydroxyl and an alkoxy radicals. Figure 11 presents the species which can be produced by decomposition of the alkoxy radicals obtained from the allylic radicals derived from the three isomers of linear hexene. All these radicals can decompose by breaking a C-C bond to give the C₃-C₅ unsaturated aldehydes which are plotted in Figure 12. Only one of these radicals derived from 1-hexene can decompose by breaking a C-H bond to give 2-hexenal, a very minor product of our study, in agreement with the fact that a C-H bond breaking requires a higher activation energy than a C(sp³)-C(sp³) bond breaking.

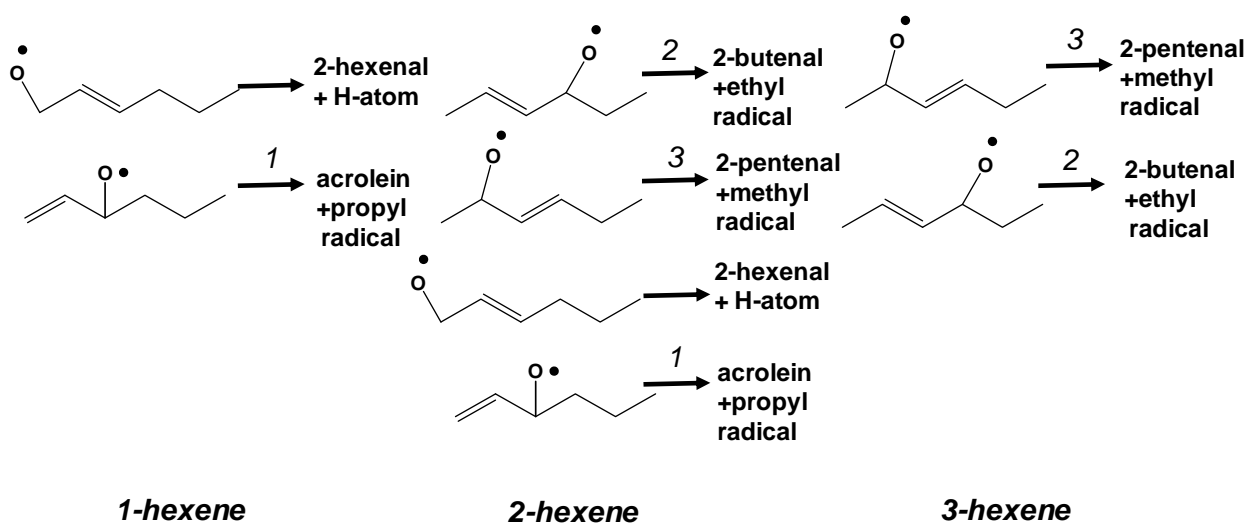


Figure 11. Decomposition of the alkoxy radicals which can be produced from the allylic radicals from the three isomers of linear hexene. C-H bond breaking is only shown where C(sp³)-C(sp³) bond breaking is not possible.

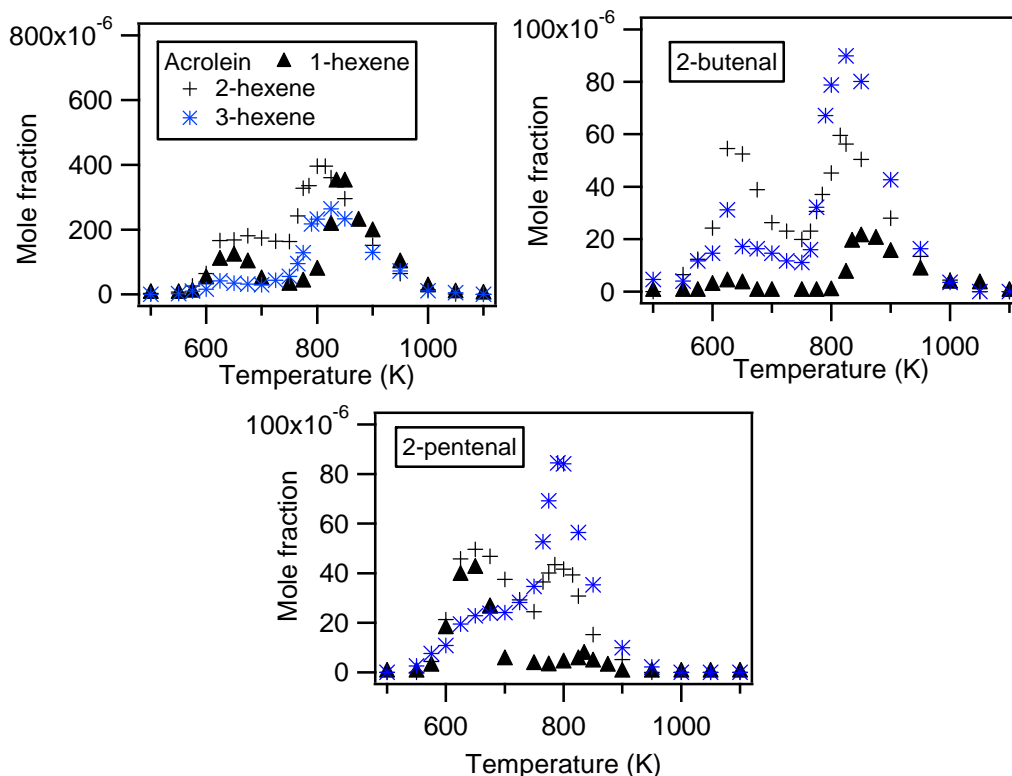


Figure 12. Comparison between the three isomers of hexene for the formation of unsaturated aldehydes which can be obtained from hexenyl hydroperoxide via pathways involving the breaking of a $C(sp^3)-C(sp^3)$ bond.

At low temperature acrolein is only significantly formed from 1- and 2-hexenes, which is in agreement with pathway 1 shown in Figure 11. The co-product of acrolein is *n*-propyl radical, a source of propene. Pathway 1 certainly explains the small amount of propene identified during the oxidation of 2-hexene between 700 and 750 K. At higher temperature, acrolein is also formed from 3-hexene, but this small aldehyde can be formed by several reactions, especially the combination of HO_2 and allyl radicals, with allyl radicals deriving from propene.

Over all the temperature range, 2-butenal is mainly formed from 2- and 3-hexenes, with only a small amount obtained from 1-hexene at high temperature. This is consistent with the pathway 2 presented in Figure 11. The co-product of 2-butenal is ethyl radical, a source of ethylene. Pathway 2 certainly explains the small amount of ethylene found during the oxidation of 2- and 3-hexenes between 700 and 750 K.

Finally above 700 K, 2-pentenal is only significantly formed from 2- and 3-hexenes, which is in agreement with pathway 3 shown in Figure 11. The co-product of 2-pentenal is the methyl radical, a

source of methane. Pathway 3 certainly explains the more significant formation of methane observed during the oxidation of 2- and 3-hexenes above 750 K compared to 1-hexene. Note that the formation of 2-pentenal is observed at low temperature from 1-hexene indicating that there should be an additional pathway forming this minor product by addition to an oxygen molecule of the common resonance stabilized allylic radical deriving from 1- and 2-hexenes.

HO₂ radicals can also react with the alkene reactants and be a source of three membered ring cyclic ethers, oxiranes, as proposed by Stark²⁹. As shown in Figure 5, the formation of significant amounts of butyloxirane and 2,3-diethyloxirane have been observed for 1-hexene and 3-hexene, respectively. This is in agreement with the reaction mechanism proposed by Stark²⁹. Only traces of methyl,propyloxirane was detected in the case of 2-hexene, while it would have been expected in larger amounts and has been easily analysed during the oxidation of *n*-hexane²⁵, using the same reactor and analytical method. Also the reaction mechanism proposed by Stark²⁹ does not explain why butyloxirane and 2,3-diethyloxirane are formed in significant amounts during the oxidation of 3-hexene and 2-hexene, respectively, as shown in Figure 5.

Finally, as shown in Figure 3, the addition of H-atoms to the double bond could be a source of hexyl radicals and then through oxygen addition to saturated ethers. While a much larger variety has been observed during the oxidation of *n*-hexane²⁵, here only the previously described oxiranes and 2,5-dimethyltetrahydrofuran were detected. As shown in Figure 5, 2,5-dimethyltetrahydrofuran can only be detected during the oxidation of 1- and 2-hexenes. Note that this ether was the one detected in largest amounts during the oxidation of *n*-hexane²⁵ and that it is mainly obtained from 2-hexyl radicals which can only be produced by H-addition to 1- and 2-hexenes.

Conclusion

This paper presents new results on the oxidation of the three isomers of linear hexene obtained in a quartz isothermal jet-stirred reactor at temperatures ranging from 500 to 1100 K and at quasi-atmospheric pressure. A discussion about the formation of some products, especially dienes, and saturated and unsaturated aldehydes, allows underlining the importance of the reactions specific to the alkene chemistry: the reaction of hydroxyalkyl radicals via or not via the Waddington mechanism and the reactions related to allylic and HO₂ radicals. Before undertaking to model these complex data, it would be important that the kinetics of these specific reactions would be better investigated, especially with the help of quantum mechanics calculations.

Acknowledgement

This study was supported by the European Commission through the “Clean ICE” Advanced Research Grant of the European Research Council.

Supporting Information Available

A table with the full experimental data is provided. This material is available free of charge via the Internet at <http://pubs.acs.org>.

References

- (1) Guibet, J.C., *Fuels and Engines*, Publications de l'Institut Français du Pétrole, Editions Technip, Paris, 1999.
- (2) Touchard, S.; Fournet, R.; Glaude, P.A.; Warth, V.; Battin-Leclerc, F.; Vanhove, G., Ribaucour, M.; Minetti, R. Modeling of the Oxidation of Large Alkenes at Low Temperature *Proc. Comb. Inst.*, **2005**, *30*, 1073–1081.
- (3) Mehl, M.; Vanhove, G.; Pitz, W.J.; Ranzi, E. Oxidation and Combustion of the n-Hexene Isomers: A Wide Range Kinetic Modeling Study *Combust. Flame*, **2008**, *155*, 756–772.
- (4) Bounaceur, R.; Warth, V.; Sirjean, B.; Glaude, P.; Fournet, R.; Battin-Leclerc, F. Influence of the Position of the Double Bond on the Autoignition of Linear Alkenes at Low Temperature *Proc. Comb. Inst.*, **2009**, *32*, 387–394.
- (5) Vanhove, G.; Ribaucour, M.; Minetti, R. On the Influence of the Position of the Double Bond on the Low-Temperature Chemistry of Hexenes *Proc. Comb. Inst.*, **2005**, *30*, 1065–1072.
- (6) Tanaka, S.; Ayala, F.; Keck, J.C., Heywood, J.B. Two-Stage Ignition in HCCI Combustion and HCCI Control by Fuels and Additives *Combust. Flame*, **2003**, *132*, 219–239.
- (7) Ribaucour, M.; Minetti, R.; Sochet, L.R. Autoignition of n-Pentane and 1-Pentene: Experimental Data and Kinetic Modeling *Proc. Combust. Inst.*, **1998**, *27*, 345–351.
- (8) Touchard, S.; Buda, F.; Dayma, G.; Glaude, P. A.; Fournet, R.; Battin-Leclerc, F. Experimental and Modeling Study of the Oxidation of 1-Pentene at High Temperature *Int. J. Chem. Kin.* **2005**, *37*, 451–463.
- (9) Prabhu, S.K.; Bhat, R.K.; Miller, D.L.; Cernansky, N.P. 1-Pentene Oxidation and its Interaction with Nitric Oxide in the Low and Negative Temperature Coefficient Regions *Combust. Flame*,

- 1996, 104, 377–390.
- (10) Mehl, M.; Pitz, W.J.; Westbrook, C.K.; Yasunaga, K.; Conroy, C.; Curran, H.J. Autoignition Behavior of Unsaturated Hydrocarbons in the Low and High Temperature Regions *Proc. Comb. Inst.*, **2011**, 33, 201–208.
- (11) Yahyaoui, M.; Djebaili-Chaumeix, N.; Dagaut, P.; Paillard, C.-E.; Gail, S. Kinetics of 1-Hexene Oxidation in a JSR and a Shock tube: Experimental and Modeling study *Combust. Flame*, **2006**, 147, 67–78.
- (12) Yahyaoui, M.; Djebaili-Chaumeix, N.; Paillard, C.-E.; Touchard, S.; Fournet, R.; Glaude, P. A.; Battin-Leclerc, F. Experimental and Modelling study of 1-Hexene Oxidation Behind Reflected Shock Waves *Proc. Comb. Inst.*, **2005**, 30, 1137–1145.
- (13) Matras, D.; Villermaux, J. Un Réacteur Continu Parfaitement Agité par Jets Gazeux pour l'Etude Cinétique de Réaction Chimiques Rapides *Chem. Eng. Sci.* **1973**, 28, 129-137.
- (14) Barhini, C.; Morajkar, P.; Shoemeacker, S.; Frottier, O.; Herbinet, O.; Glaude, P.A.; Battin-Leclerc, F.; Fittschen, C. Experimental and Modeling Study of the Oxidation of *n*-Butane in a Jet Stirred Reactor using cw-CRDS Measurements *Phys. Chem. Chem. Phys.*, **2013**, 15, 19686-19698.
- (15) Herbinet, O.; Husson, B., Serinyel, Z.; Cord, M.; Warth, V.; Fournet, R., Glaude, P.A.; Sirjean, B.; Battin-Leclerc, F.; Wang, Z.; Xie, M.; Cheng, Z.; Qi, F. Experimental and Modeling Investigation of the Low-Temperature Oxidation of *n*-Heptane *Combust. Flame*, **2012**, 159, 3455-3471.
- (16) Husson, B.; Herbinet, O.; Glaude, P.A.; Ahmed, S.S.; Battin-Leclerc, F. Detailed Product Analysis during the Low and Intermediate Temperature Oxidation of Ethylcyclohexane *J. Phys. Chem. A*, **2012**, 116, 5100-5111.
- (17) Herbinet, O., Battin-Leclerc, F., Bax, S., Gall, H.L., Glaude, P.-A., Fournet, R., Zhou, Z., Deng, L., Guo, H., Xie, M., Qi, F. Detailed Product Analysis during the Low Temperature Oxidation of *n*-Butane *Phys. Chem. Chem. Phys.*, **2011**, 13, 296-308.
- (18) Battin-Leclerc, F. Detailed Chemical Kinetic Models for the Low Temperature Combustion of Hydrocarbons with Application to Gasoline and Diesel Fuel *Prog. Energ. Combust. Sci.* **2008**, 34, 440–498.
- (19) Battin-Leclerc, F., Herbinet, O., Glaude, P.-A., Fournet, R., Zhou, Z., Deng, L., Guo, H., Xie, M., Qi, F. Experimental Confirmation of the Low-Temperature Oxidation Scheme of Alkanes, *Angew. Chem. Int. Ed.*, **2010**, 49, 3169–3172.
- (20) Montgomery, J.A.; Frisch, M.J.; Ochterski, J.W.; Petersson, G.A. A Complete Basis Set Model Chemistry. VI. Use of Density Functional Geometries and Frequencies *J. Chem. Phys. A* **1999**,

110, 2822-2827.

- (21) Frisch, M. J.; Trucks, G. W.; Schlegel, H. B.; Scuseria, G. E.; Robb, M. A.; Cheeseman, J. R.; Scalmani, G.; Barone, V.; Mennucci, B.; Petersson, G. A. et al., Gaussian, Revision B.01 Wallingford CT, 2009.
- (22) Cord, M., Husson, B., Lizardo Huerta, J.C., Herbinet, O., Glaude, P.-A., Fournet, R., Sirjean, B., Battin-Leclerc, F., Ruiz-Lopez, M., Wang, Z. et al. Improvement of the Modelling of the Low-Temperature Oxidation of n-Butane – Study of the Primary Reactions *J. Phys. Chem. A*, **2012**, *116* (50), 12214–12228.
- (23) Stark, M.S., Waddington, R.W. Oxidation of Propene in the Gas Phase *Int. J. Chem. Kin.* **1995**, *27*, 123–51.
- (24) Welz, O.; Savee, J.D.; Eskola, A.J.; Sheps, L.; Osborn, D.L.; Taatjes, C.A. Low-Temperature Combustion Chemistry of Biofuels: Pathways in the Low-Temperature (550–700 K) Oxidation Chemistry of *iso*Butanol and *tert*-Butanol *Proc. Combust. Inst.*, **2013**, *34*, 493-500.
- (25) Serinyel, Z.; Herbinet, O.; Glaude, P.-A.; Warth, V.; Battin-Leclerc, F., Wang, Z.D.; Cheng, Z.J.; Qi, F. An Experimental and Modeling Investigation of the Low Temperature Oxidation of n-Hexane, 2-methyl-Pentane and 3-methyl-Pentane, *Proceeding of the 8th Mediterranean Symposium*, Çeşme, Izmir, Turkey, September 8-13, 2013.
- (26) Dibble, T.S.; Sha, Y.; Thornton, W.F.; Zhang, F. Cis–trans Isomerization of Chemically Activated 1-methylAllyl Radical and Fate of the Resulting 2-Buten-1-peroxy radical, *J. Phys. Chem. A*, *116* (2012) 7603-7614.
- (27) Griffiths, J. F.; Hughes, K. J.; Porter, R. The Role and Rate of Hydrogen Peroxide Decomposition During Hydrocarbon Two-Stage Autoignition *Proc. Combust. Inst.* **2005**, *30*, 1083-1091.
- (28) Bahrini, C., Herbinet, O., Glaude, P.-A., Schoemaeker, C., Fittschen, C., Battin-Leclerc, F., Quantification of Hydrogen Peroxide during the Low-Temperature Oxidation of Alkanes *J. Am. Chem. Soc.*, **2012**, *134*, 11944–11947.
- (29) Stark, M.S. Epoxidation of Alkenes by Peroxyl Radicals in the Gas Phase: Structure-Activity Relationships *J. Phys. Chem. A*, **1997**, *101*, 82296-82301.